Computational design of an automotive twist beam

Aalae Benki, Abderrahmane Habbal, Gaël Mathis

HAL Id: hal-01405109
https://hal.inria.fr/hal-01405109

Submitted on 29 Nov 2016

Computational design of an automotive twist beam

Benki Aalae[a,*], Habbal Abderrahmane[b], Mathis Gael[c]

[a]INRIA Sophia Antipolis, OPALE Project Team, 2004 Route des Lucioles, 06902 Sophia Antipolis, France
[b]University Nice Sophia Antipolis, Mathematics Department, 28 Avenue de Valrose, 06103 Nice Cedex 2, France
[c]ArcelorMittal Global R&D, route de St. Leu, 60761 Montataire Cedex, France

Abstract

In recent years, the automotive industry has known a remarkable development in order to satisfy the customer requirements. In this paper, we will study one of the components of the automotive which is the twist beam. The study is focused on the multicriteria design of the automotive twist beam undergoing linear elastic deformation (Hooke's law). Indeed, for the design of this automotive part, there are some criteria to be considered as the rigidity (stiffness) and the resistance to fatigue. Those two criteria are known to be conflicting, therefore, our aim is to identify the Pareto front of this problem. To do this, we used a Normal Boundary Intersection (NBI) algorithm coupling with a radial basis function (RBF) metamodel in order to reduce the high calculation time needed for solving the multicriteria design problem. Otherwise, we used the free form deformation (FFD) technique for the generation of the 3D shapes of the automotive part studied during the optimization process.
© 2016 Society of CAD/CAM Engineers. Publishing Services by Elsevier. This is an open access article under the CC BY-NC-ND license (http://creativecommons.org/licenses/by-nc-nd/4.0/).

Keywords: Automotive twist beam; Multicriteria design; Free form deformation; Normal boundary intersection; Radial basis function

1. Introduction

In the automotive industry, and particularly, in the shape design optimization field, the most of problems faced are multicriteria ones. Indeed, one way to solve these problems is to identify the Pareto front. To do this, there are often two issues to confront, the first one is how to reduce the computational time required by the conventional methods used to solve this kind of optimization problem, and the second one is how can we generate the 3D shapes of the automotive part studied in the optimization process. To overcome the first issue, it is necessary to couple methods for capturing the Pareto front with metamodels aimed at cheap costs' evaluations. For the second issue, there are several versions of FFD technique used to do this [1–3].

The Twist beam suspension (Fig. 1) is widely used as rear wheel suspension systems for front wheel driven passenger vehicles, it is composed of several components such as swing or trailing arms, bushings and the twist beam which is the object of our study.

For our work, we focus on optimizing the shape of a twist beam undergoing linear elastic deformation (Hooke's law) [4–6] to improve certain mechanical criteria such as the rigidity and the resistance to fatigue of this automotive part (Fig. 1). Firstly, for the identification of the Pareto front with a reasonable calculation time, we use the (NBI RBF) algorithm built using a coupling between the NBI method [7–10] and the RBF metamodel [11–15], the idea is to lead optimization with the metamodel and only do the exact evaluations of the metamodel obtained solutions [16–20]. Secondly, for the generation of 3D shapes during the optimization process, we use a developed version of the free form deformation technique using radial basis functions (FFD RBF) [21–23].

2. Methodology

This section will be divided into three parts, the first one is a reminder of the multicriteria optimization basics and fundamentals, then, we present the two main methods used

---

*Corresponding author.

Peer review under responsibility of Society of CAD/CAM Engineers.

in our work which are the NBI RBF coupling and the FFD RBF deformation technique. The first one will be briefly presented, then, we give a complete description of the second one.
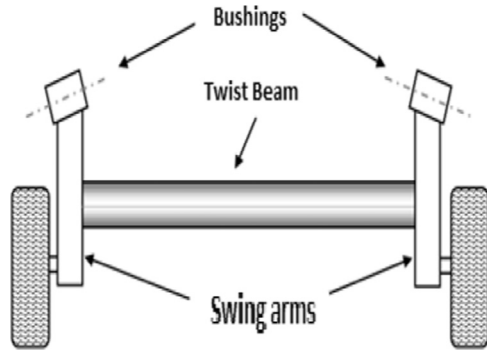

Fig. 1. Example of a typical twist beam suspension [24].

2.1. Multicriteria optimization and pareto optimality

A multicriteria optimization problem is given as follows:

$$\min_{x} F(x) = \left(f_1(x), f_2(x), \ldots, f_m(x) \right)^T,$$

$$m \geq 2 \text{ Subject to } \begin{cases} g_j(x) \geq 0, & j = 1, \ldots, J \\ p_h(x) = 0, & h = 1, \ldots, H \\ x^{lower} \leq x \leq x^{upper} \end{cases} \quad (1)$$

where m, J and H are the total numbers of the objective functions, the inequality (g_j) and equality constraints (p_h), respectively.

The Pareto front is defined as the set of non-dominated designs. In the objective space, $x^* \in D$ is non-dominated if there is no other point, $x^* \in D$, such that

$$f_i(x) < f_i(x^*), \quad i = 1, \ddot{,} m$$
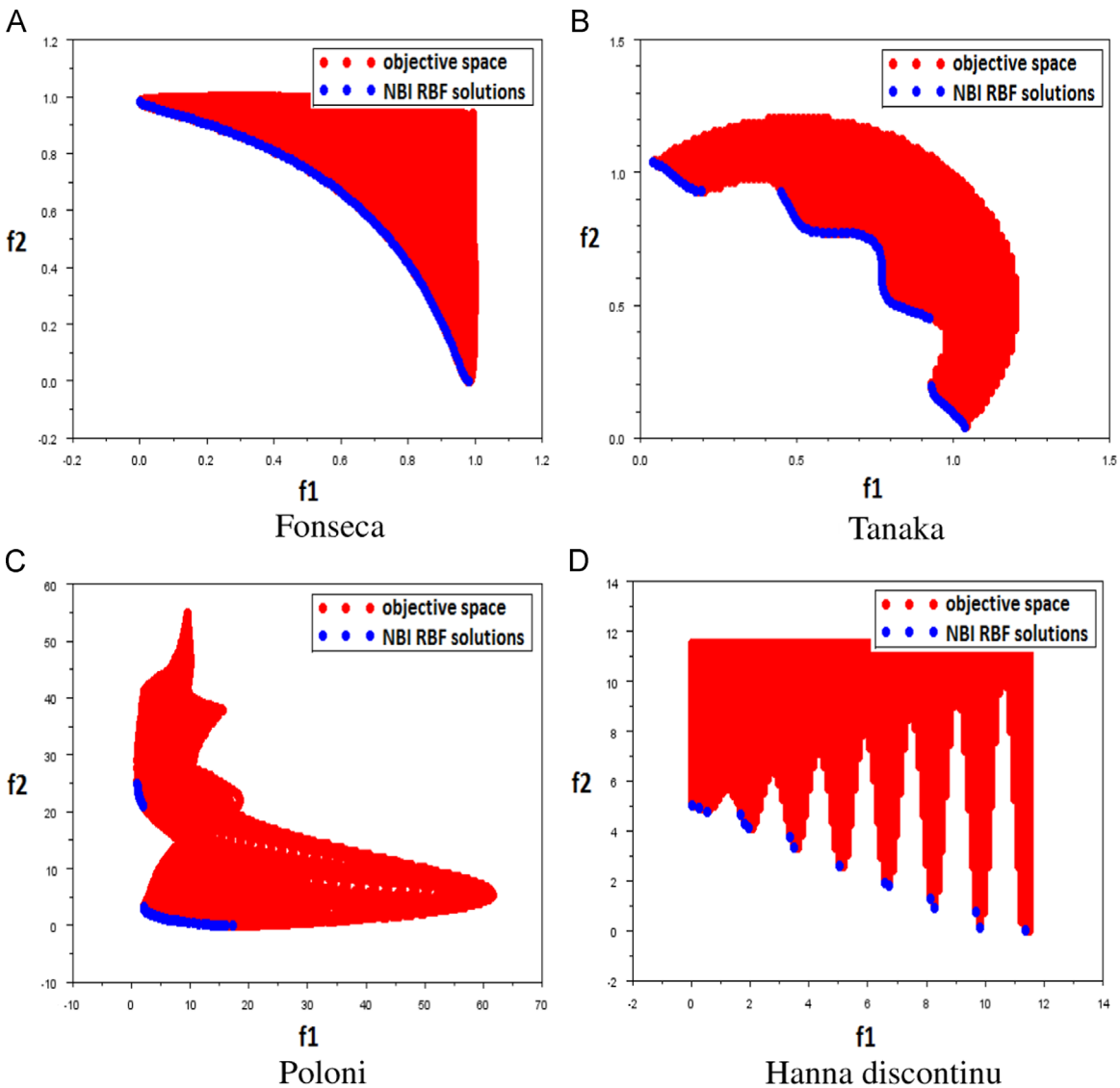
with strict inequality for at least one index.

Fig. 2. The results obtained by the NBI RBF coupling (blue points) after filtering dominated points for different academic problems.

2.2. The NBI RBF coupling

We had presented previously the algorithm of the NBI RBF coupling in detail [25], which is why we give below just the key points of this coupling. Let us consider the following multicriteria optimization problem ($m=2$):

$$\min_{x} F(x) = \left(f_1(x), f_2(x)\right)^T$$

$$\text{Subject to } \begin{cases} g_j(x) \geq 0, & j = 1, \ldots, J \\ p_h(x) = 0, & h = 1, \ldots, H \\ x^{lower} \leq x \leq x^{upper} \end{cases} \quad (2)$$

Let $\tilde{f}_1(x)$ and $\tilde{f}_2(x)$ the approximations obtained from a classical RBF for the initial functions f_1 and f_2, respectively.

We will solve the following problem equivalent to the original one (2), replacing the objective functions with their approximate functions constructed using the RBF metamodel,

by the NBI method:

$$\min_{x} \tilde{F}(x) = \left(\tilde{f}_1(x), \tilde{f}_2(x)\right)^T$$

$$\text{Subject to } \begin{cases} g_j(x) \geq 0, & j = 1, \ldots, J \\ p_h(x) = 0, & h = 1, \ldots, H \\ x^{lower} \leq x \leq x^{upper} \end{cases} \quad (3)$$

Fig. 2 presents the solutions obtained by the NBI RBF coupling after filtering dominated points for some academic test cases [27] and it clearly shows the effectiveness of the algorithm developed for capturing the Pareto front.

To show the effectiveness of our developed algorithm at the computing time reduction (i.e. cost evaluation of objective functions), we solve the problems "A, B, C and D" with our new algorithm "NBI RBF coupling" and the conventional method NBI without coupling, then, we make a comparison
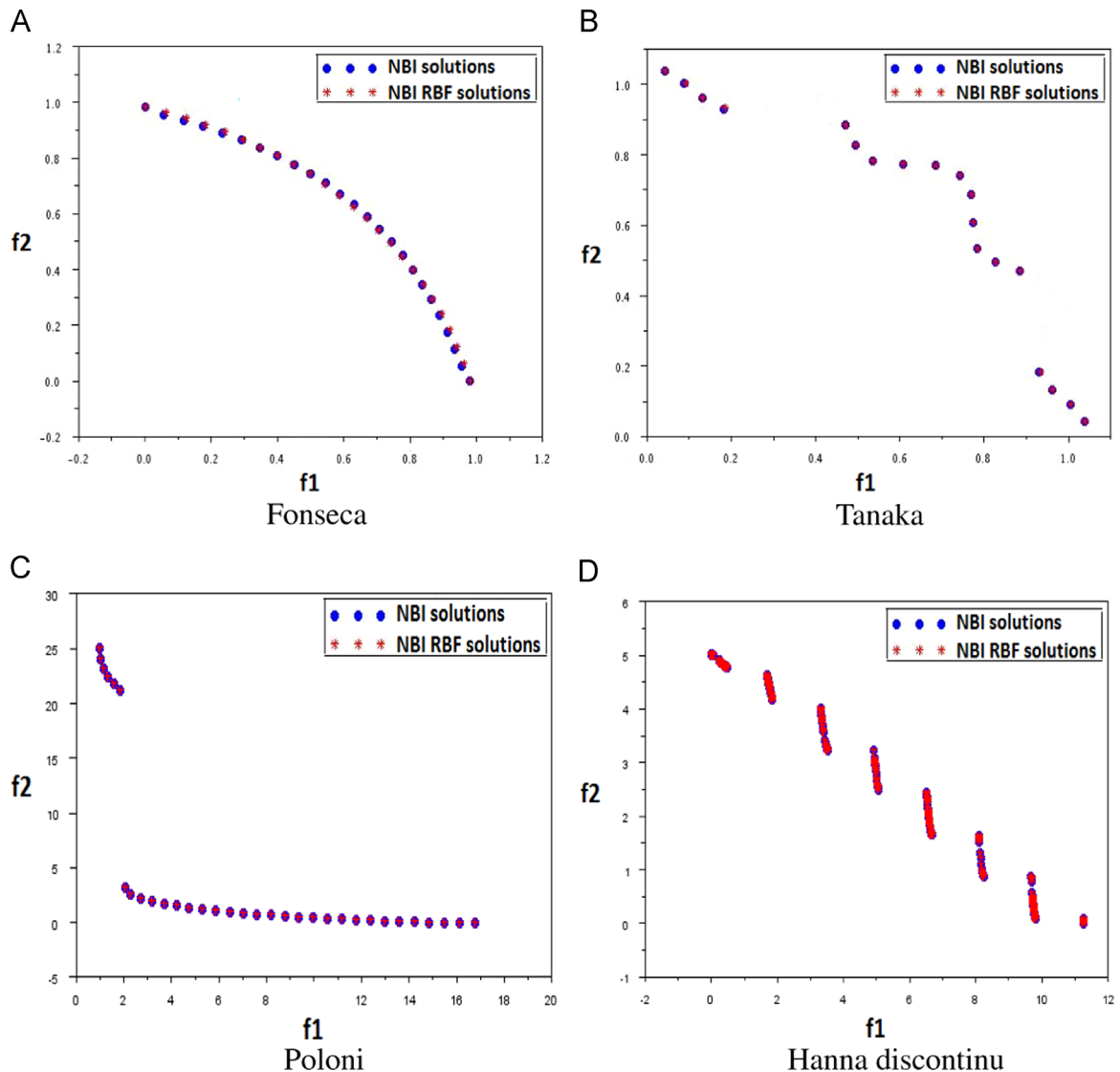

Fig. 3. Comparison between the results obtained by NBI RBF approach (in red), and the exact solutions NBI (in blue) after filtering dominated points.

between the results obtained (the number of functions' call needed by each method).

The results, Fig. 3 and Table 1, show that the coupling NBI RBF converges to the Pareto frontier with an approximately 58%, 94%, 80% and 84% fewer number of objective functions' calls compared to a conventional NBI for Fonseca, Tanaka, Poloni and Hanna problem, respectively.

2.3. The FFD RBF technique

In this section, we present a version of the free form deformation (FFD) which is a geometric technique used to model simple deformations of rigid objects using a technique based on radial basis functions (RBF). These mathematical functions can be used for the creation of a smooth interpolation between values known only to a discrete set of positions.

Let $f : \mathbb{R}^3 \to \mathbb{R}$ be a scalar-valued function.

Suppose that this function is known on a M distinct discrete set of points in three dimensional space $(\mathbf{x}_i, f(\mathbf{x}_i))$.

Let $g(r_i) : \mathbb{R} \to \mathbb{R}$ be a radial basis function where r_i is the distance from the point $\mathbf{x}$ we seek to evaluate and $\mathbf{x}_i$ already known (one among the M points). The function F_{RBF} provides us a way to create a smooth interpolation function of f in the whole field of $\mathbb{R}^3$. F_{RBF} is written as a sum of M estimates of the radial basis function $g(r_i)$ and it is given by the following formulation:

$$F_{RBF}(\mathbf{x}) = \sum_{i=1}^{M} w_i g(\| \mathbf{x} - \mathbf{x}_i \|) + c_0 + c_1 x + c_2 y + c_3 z, \quad \mathbf{x} = (x, y, z)$$

(4)

where w_i are scalar coefficients and the last four terms are a first degree polynomial with coefficients c_0, c_1, c_2 and c_3, these terms describe an affine transformation which can be achieved by the radial functions.

Since the M known values of the function $f(x_i, y_i, z_i) = F_i$, we can assemble a linear system of equations of order $M+4$:

$$\mathbf{GA} = \mathbf{F}$$

(5)

where $\mathbf{F} = (F_1, F_2, ..., F_M, 0, 0, 0, 0)^T$, $\mathbf{A} = (w_1, w_2, ..., w_M, c_0, c_1, c_2, c_3)^T$ and $\mathbf{G}$ is a matrix of order $(M+4) \times (M+4)$ defined as follows:

$$\mathbf{G} = \begin{bmatrix} g_{11} & g_{12} & \bullet & \bullet & \bullet & g_{1M} & 1 & x_1 & y_1 & z_1 \\ g_{21} & g_{22} & \bullet & \bullet & \bullet & g_{2M} & 1 & x_2 & y_2 & z_2 \\ \bullet & \bullet & \bullet & \bullet & \bullet & \bullet & \bullet & \bullet & \bullet & \bullet \\ \bullet & \bullet & \bullet & \bullet & \bullet & \bullet & \bullet & \bullet & \bullet & \bullet \\ \bullet & \bullet & \bullet & \bullet & \bullet & \bullet & \bullet & \bullet & \bullet & \bullet \\ g_{M1} & g_{M2} & \bullet & \bullet & \bullet & g_{MM} & 1 & x_M & y_M & z_M \\ 1 & 1 & \bullet & \bullet & \bullet & 1 & 0 & 0 & 0 & 0 \\ x_1 & x_2 & \bullet & \bullet & \bullet & x_M & 0 & 0 & 0 & 0 \\ y_1 & y_2 & \bullet & \bullet & \bullet & y_M & 0 & 0 & 0 & 0 \\ z_1 & z_2 & \bullet & \bullet & \bullet & z_M & 0 & 0 & 0 & 0 \end{bmatrix}$$

(6)

where $g_{ij} = g(\| \mathbf{x}_i - \mathbf{x}_j \|)$. For the choice of the radial basis function, there are several known in the scientific literature. For our work, we use the gaussian function $g(t) = \exp(-(kt)^2)$ with $k=3$. Now we can easily solve Eq. (5) to obtain the $M+4$ coefficients to be used in the expression (4) for the interpolation.

Table 1
Functions call number required by NBI and NBI RBF methods.

Problem	Method used	Prescribed pareto points (N)	Functions calls
Fonseca	NBI	25	305
	NBI RBF	25	128
Tanaka	NBI	25	942
	NBI RBF	25	50
Poloni	NBI	50	668
	NBI RBF	50	128
Hanna	NBI	100	1024
	NBI RBF	100	162

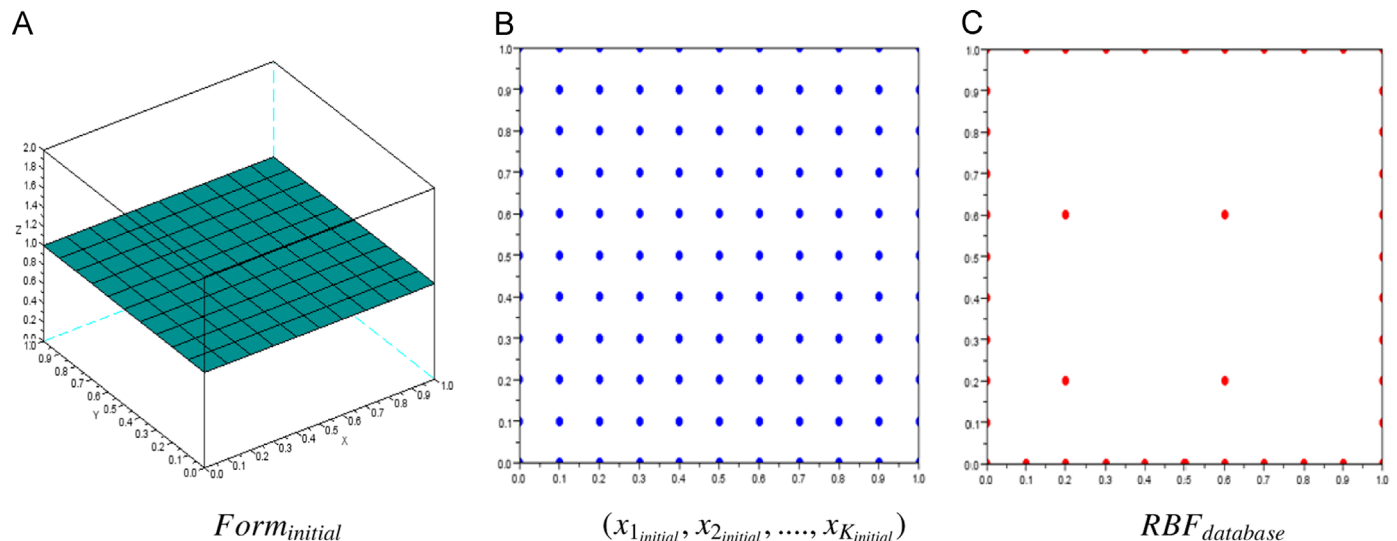$Form_{initial}$ $\qquad$ $(x_{1_{initial}}, x_{2_{initial}}, ..., x_{K_{initial}})$ $\qquad$ $RBF_{database}$

Fig. 4. (A) A flat surface, (B) all the points constituting the flat surface (blue points, $K=121$), (C) the points used for interpolation FFD RBF (red points, $M=44$).

A
B

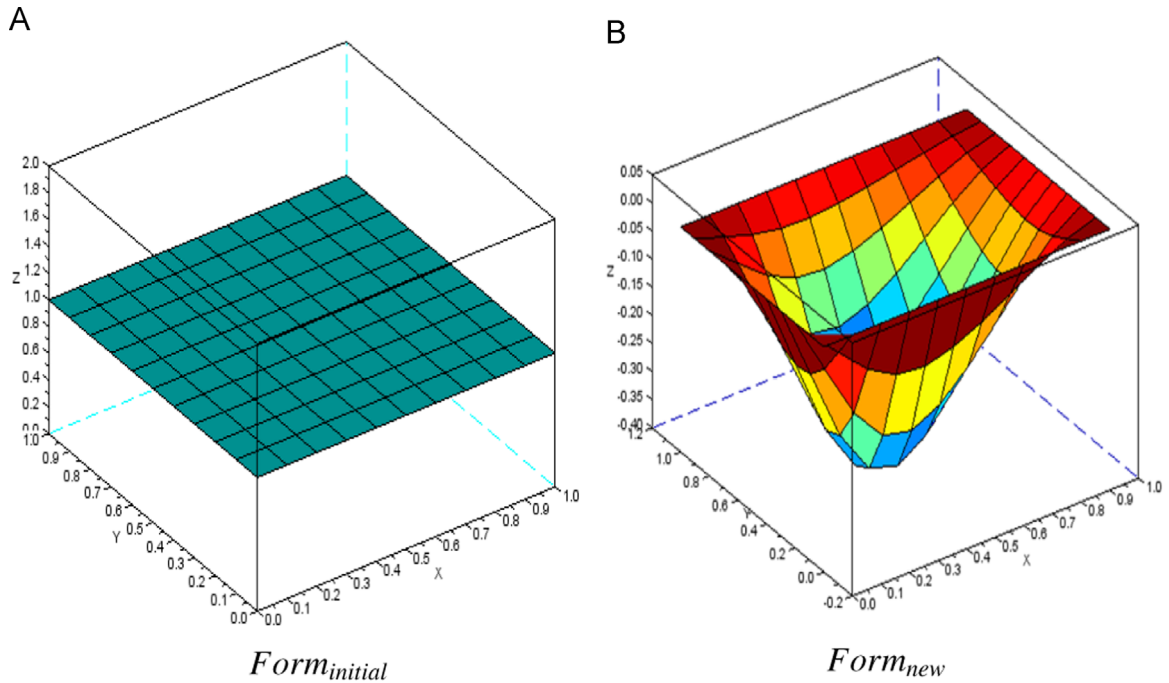$Form_{initial}$ $Form_{new}$

Fig. 5. Example of the application of the FFD RBF technique to a flat surface (A) and the deformed surface obtained (B).
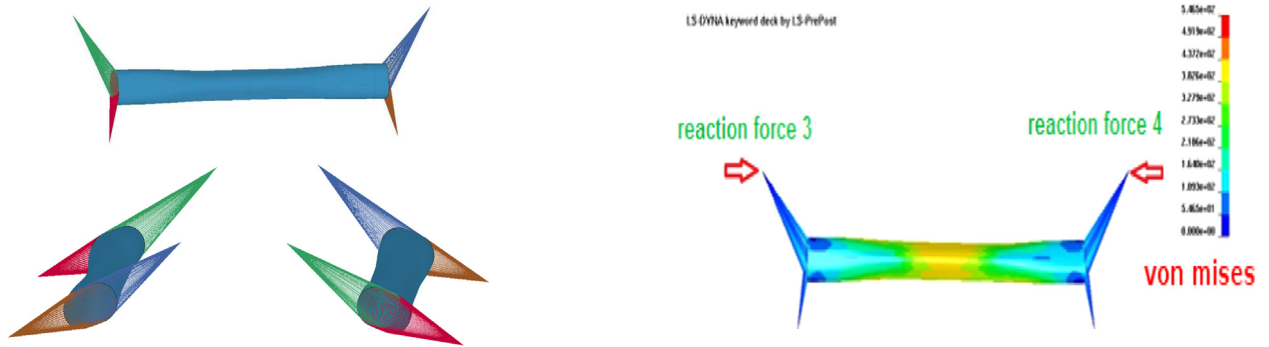

Fig. 6. The initial shape of the twist beam used—visualization from different sides by the software Ls Dyna.

Fig. 7. Two criteria to be optimized "FR_{34} vs VM": the first criterion and the second one present the rigidity and the resistance to fatigue, respectively.

2.4. Illustration of the FFD RBF technique

Let $Form_{initial}$ a 3D geometry which we seek to deform

$$Form_{initial} = (x_{1_{initial}}, x_{2_{initial}}, x_{3_{initial}}, \ldots, x_{K_{initial}}). \qquad (7)$$

First, we choose a set of M points, $RBF_{database}$, from the initial geometry

$$RBF_{database} = (x_{1_{initial}}, x_{2_{initial}}, \ldots, x_{M_{initial}}) \in Form_{initial} \quad (M < K). \qquad (8)$$

Then we start with the deformation of these points (deformation=moving points in 3D space), this deformation is represented by a vector describing the 3D displacement of $\mathbf{u}_i$ the points chosen which has been positioned at $\mathbf{x}_{i_{initial}}$ in the initial geometry. The new position of the $RBF_{database}$ points is described by the vectors:

$$RBF_{database_{newposition}} = (x_{1_{new}}, x_{2_{new}}, \ldots, x_{M_{new}}) \qquad (9)$$

where $x_{i_{new}} = x_{i_{initial}} + \mathbf{u}_i (i = 1, \ldots, M)$. Let $\mathbf{x}_i = x_{i_{initial}} = (x_i, y_i, z_i)$ and $\mathbf{u}_i = (u_i^x, u_i^y, u_i^z)(i = 1, \ldots, M)$. We consider the following three linear systems:

$$\begin{cases} \mathbf{GA}_x = (u_1^x, u_2^x, \ldots, u_M^x, 0, 0, 0, 0)^T \\ \mathbf{GA}_y = (u_1^y, u_2^y, \ldots, u_M^y, 0, 0, 0, 0)^T \\ \mathbf{GA}_z = (u_1^z, u_2^z, \ldots, u_M^z, 0, 0, 0, 0)^T \end{cases} \qquad (10)$$

where $\mathbf{G}$ is assembled as described in the matrix (6). The solutions of $\mathbf{A}_x$, $\mathbf{A}_y$ and $\mathbf{A}_z$ give us the interpolation coefficients for the predicted displacement in the three directions (x, y and z) of the expression (4), F_{RBF_x}, F_{RBF_y} and F_{RBF_z} respectively. Then the new geometry $Form_{new}$ of the initial geometry $Form_{initial}$ is defined as follows:

$$Form_{new} = (x_{i_{new}})_{i=1,\ldots,K} \qquad (11)$$

where

$$x_{i_{new}} = \begin{cases} \mathbf{x}_i + \mathbf{u}_i & \text{if } \mathbf{x}_i \in RBF_{database} \\ \mathbf{x}_i + (F_{RBF_x}(\mathbf{x}_i), F_{RBF_y}(\mathbf{x}_i), F_{RBF_z}(\mathbf{x}_i)) & \text{else} \end{cases}$$

To illustrate the FFD RBF technique presented above, we present a simple example which is the deformation of a flat surface (Fig. 4). In fact, to deform the surface (A), we move only the points selected, and we used the FFD technique that allows us to have an approximation for the displacement of all the other points (Fig. 5).
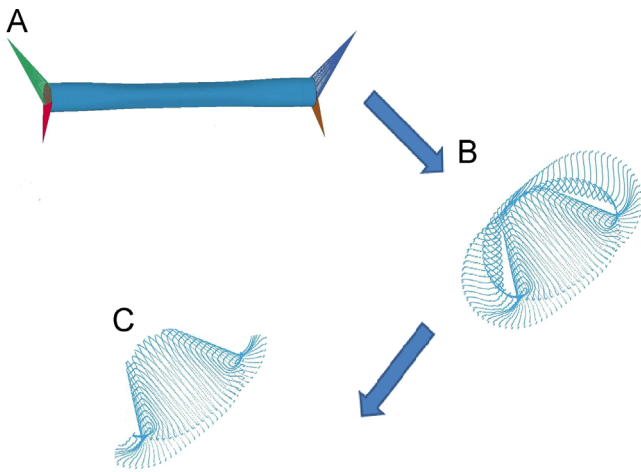

Fig. 8. (a) Visualization of the automotive twist beam, (b) zoom in to highlight the belly of the automotive twist beam on the LSprepost LSDYNA software, (c) the belly of the twist beam.

Since the radial basis functions $g(t)$ do not have a compact support, the RBF approximation moves all the nodes around, even though with a very small magnitude. We are then led to enforce a null displacement at the boundary parts which are not subject to deformation. In our example, 40 points are used in order to get vanishing RBF approximation near the fixed boundary.

3. Shape optimization of an automotive twist beam

3.1. Motivation

For the design of the automotive twist beam, it is important to avoid permanent plastic deformation, in fact, its design must be studied so as to ensure that the level of stresses does not reach the elastic limit of the material. Hence the necessity to seek new geometry with more rigidity (the first criterion to be optimized) [28]. Similarly, it is essential to maximize the resistance to fatigue of the twist beam which is its ability to withstand a repeatedly applied load without failure (the second criterion to be optimized) [29,30].

The aim of this work is to seek to maximize both the rigidity and the resistance to fatigue of this automotive part (Fig. 6).

3.2. Calculation of criteria

In this study, the FEA code, LS-DYNA software, was used to model the automotive twist beam and performs the calculations of deformed linear elasticity in order to determine the criteria to be optimized. LS-DYNA is an explicit and implicit
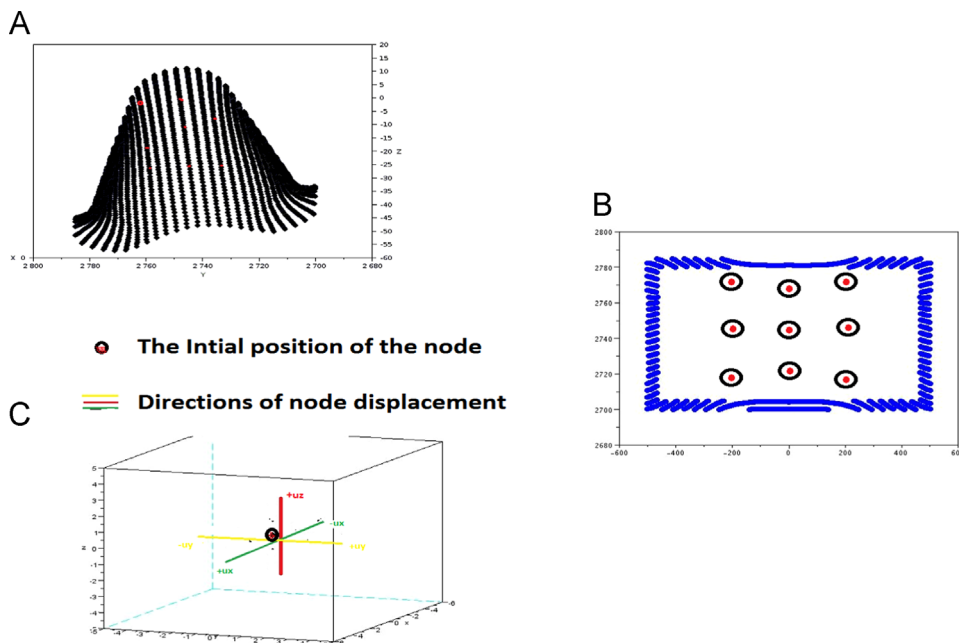

Fig. 9. Design variable: (a) extraction of the twist beam belly, (b) a 2D projection of the 3D nodes through the belly, the blue nodes are fixed and red ones are used for the generation of new profiles by using the FFD method, (c) the displacements of the nine points along the three directions which present our real design variable with 3 components.
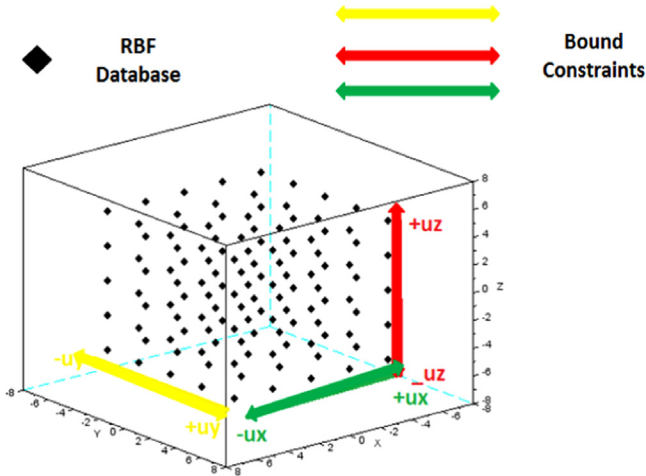
Fig. 10. The choice of the database elements to build the RBF metamodel.

Table 2
Time required for the different functions' call, (***) = (*)+(**), (d=day, h=hour, min=minute).

N	Total time***	Objective function		Approximated function	
		Call number	Time required**	Call number	Time required*
6	1d 20 h 15 min	131	1d 19 h 29 min	192	46 min
12	1d 21 h 50 min	137	1d 21 h 04 min	390	46 min
25	2d 01 h 52 min	150	2d 01 h 04 min	788	48 min
50	2d 09 h 56 min	175	2d 09 h 08 min	1584	48 min

Finite Element program dedicated to the analysis of highly non-linear physical phenomena.

Fig. 7 shows the criteria to optimize that the first criterion, is the level of rigidity, will be reviewed by an Euclidean norm of reactions at the supports − FR_{34} and the second criterion will be assessed indirectly by the level of stress (Von Mises) − VM [31,32].

The Von Mises stress σ^i_{Vmises} is calculated on all elements P_i of the twist beam. Our goal is to minimize the maximum value of the stress on the entire twist beam:

$$VM = \max_i \sigma^i_{Vmises}, \quad i = 1 : p \tag{12}$$

where p is the total number of the twist beam elements (P_i).

The two forces FR_3 and FR_4 are reaction forces exerting their actions at two points (3 and 4) and they have almost the same value with two different signs (+ and −). Our goal is to maximize these two values, for this, we have defined the following criterion:

$$FR_{34} = \sqrt{FR_3^2 + FR_4^2} \tag{13}$$

FR_{34} is the magnitude of the reaction or torsional force to an imposed displacement at the nodes' number 3 and 4. The solver LS-DYNA takes into account the ratio (reaction force)/ (imposed displacement) per angular unit and the distance between nodes 3 and 4, to compute the torsional rigidity. Thus, maximization of the latter amounts to maximize FR_{34}.

3.3. Presentation of the optimization framework

The goal is to figure out a new design of the twist beam, which satisfies a FR_{34} value bigger and a VM value smaller than the FR_{34} and VM of the initial shape respectively. Our initial shape has 546 MPa for the Von Mises constraint and a torsion reaction force of 2460 N. We will use our developed approach of optimization which allows us to set the parameters of the shape by using the free form deformation technique with radial basis function (FFD RBF) and then optimizing under bound constraints.

We start by the representation of the characteristics related to shape optimization (design variable, constraints, metamodel database and multicriteria optimization formula).

3.3.1. Design variable

The twist beam is divided into two parts, the belly of the twist beam (Fig. 8(c)) which can be considered as the design variable and the rest of the twist will be fixed.

The belly (the variable part of the shape) is parameterized by nine control points (9 points), and during the optimization process, each point will move according to the three directions (x, y, z).

Let $\mathbf{u}_i = (u_i^x, u_i^y, u_i^z)_i = 1, \ldots, 9$ be the displacement of the nine points.

In order to formulate the problem in a simple way, we decided that the displacements for the nine points will be the same and like that, the design variable has only three components which are the displacement of the nine points along the three directions:

$$\mathbf{u}_i = (u_i^x, u_i^y, u_i^z)_{i=1,\ldots,9} = (u^x, u^y, u^z) \tag{14}$$

3.3.2. Design constraints and metamodel database

Let $\varphi_0 = (\varphi_{01}, \varphi_{02}, \varphi_{03})$ be the initial shape of the twist beam, and u^x, u^y and u^z a positive offset respectively (Fig. 9). Then, we choose the bound constraints as follows:

$$*\varphi^{lower} = (\varphi_{01} - u^x, \varphi_{02} - u^y, \varphi_{03} - u^z)$$
$$*\varphi^{upper} = (\varphi_{01} + u^x, \varphi_{02} + u^y, \varphi_{03} + u^z)$$

Now we have the design variable with three components, and each component is a displacement, then, we choose 5 displacement values for each one (for example, the selected values for the displacement along the x-direction are $(-u^x, -u^x/2, 0, u^x/2, u^x)$ and similarly for the displacement along y- and z-directions) (Fig. 10).

With three components and for each variable five different positions, so we have a set of 125 points, each point representing a given shape of the twist beam. Then, for each point, we calculate the exact value of two criteria FR_{34} and VM. These
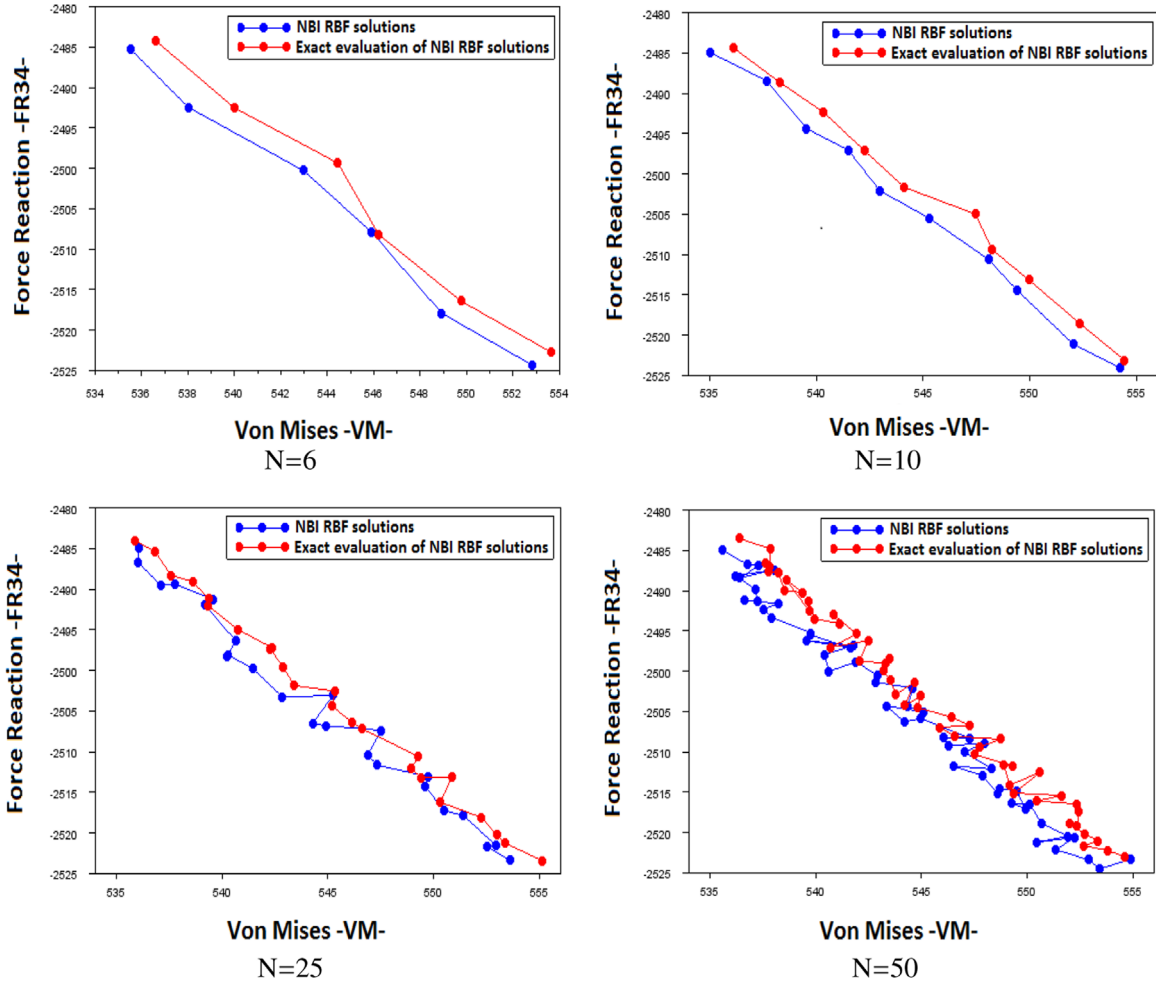
Fig. 11. Comparison between the results obtained by NBI RBF approach (in blue), and the exact cost evaluation of these results (in red).
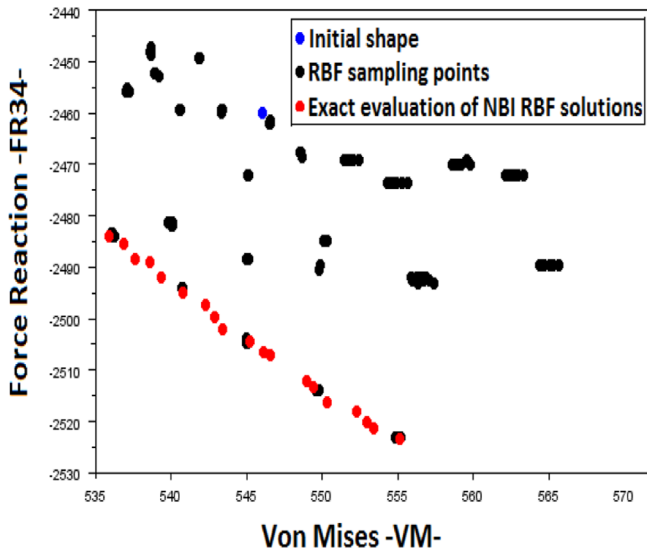

Fig. 12. Superposition of optimization results of 3D shape of the twist beam obtained by our NBI RBF approach after filtering (in red), the RBF database (in black) and the initial solution (in blue).

values present the database allowing us to build the RBF metamodel for each criterion, and the optimization problem will be studied using these metamodels.

3.3.3. Optimization formula

Knowing the criteria to be optimized and the constraints to be respected, we can write our optimization problem in the following mathematical formula:

$$\max_{\varphi = (\varphi_{axx},\varphi_{ayy},\varphi_{azz})} FR_{34}\left(\varphi\right) \Big/ \min_{\varphi = (\varphi_{axx},\varphi_{ayy},\varphi_{azz})} VM(\varphi)$$

$$\text{Subject to } (D\ twist)\{\varphi^{lower} \leq \varphi \leq \varphi^{upper} \qquad (15)$$

3.3.4. Optimization results

For $u^x = 5$; $u^y = 3$ et $u^z = 2$, we computed an approximate Pareto front for the FR_{34} and VM costs using the NBIRBF coupling. For a prescribed number of Pareto points N, we show the overall time and total number of exact and surrogate evaluations needed in Table 2 and the optimization results are shown in Fig. 11.
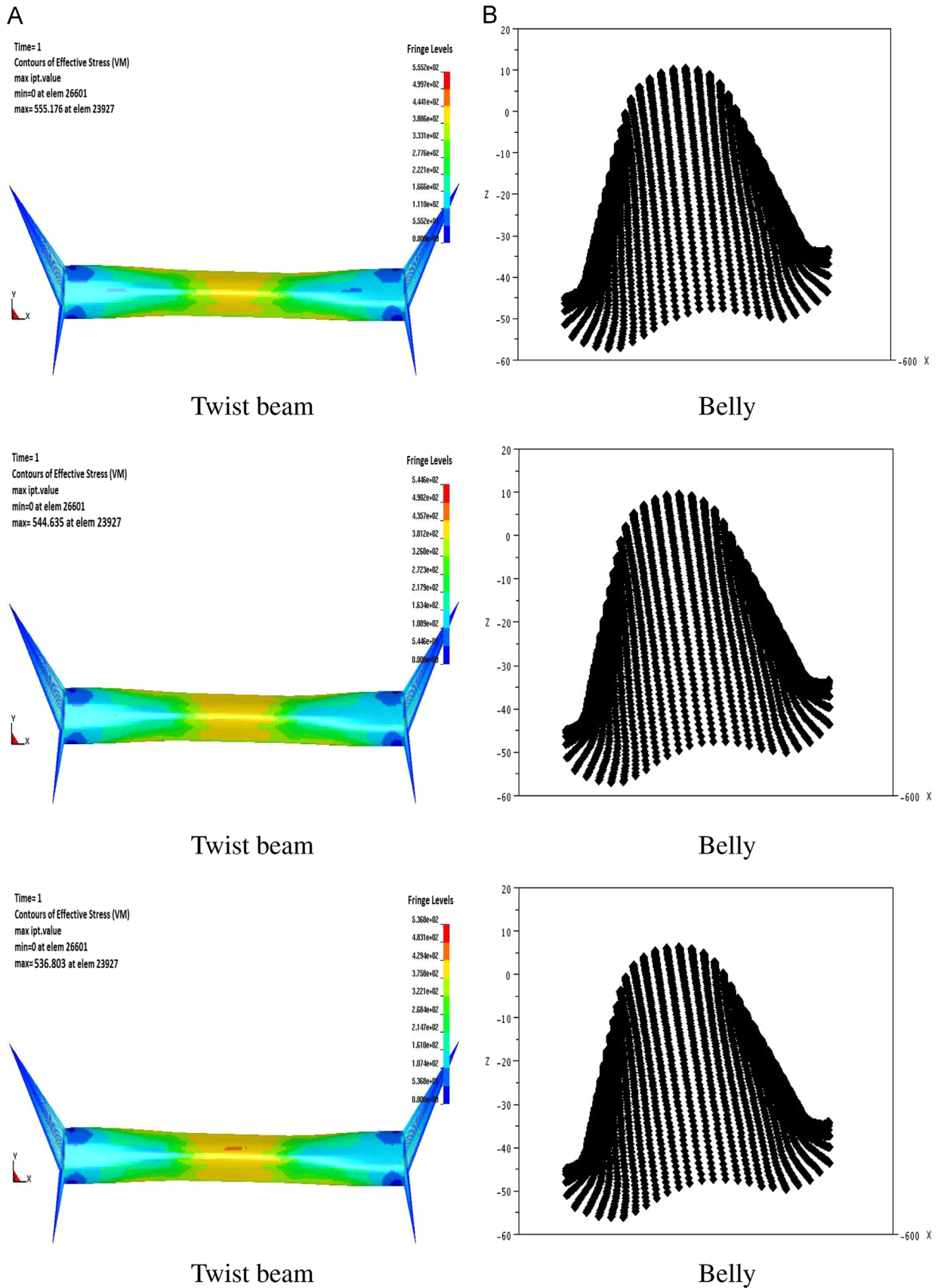
Fig. 13. New profiles of the twist beam captured by the approach developed "NBI RBF coupling": (a) the complete design of the automotive twist beam and (b) the belly of this twist beam.

Table 3
Summary of new designs 1, 2, and 3.

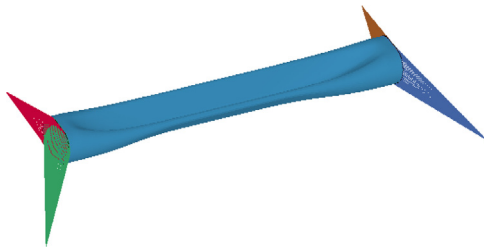| Profiles	Criteria values	
	VM (MPa)	FR_{34} (N)
Original design	546	2460
Profile (1)	555.176	2523
Profile (2)	544.635	2504
Profile (3)	536.803	2486

Fig. 14. Visualization of an optimized twist beam shape – Profile 2.

3.3.5. Results discussion

We discuss the results according to the following points:

- A simple comparison between the results obtained by our approach and the accurate evaluation of these solutions, Fig. 11, allows us to assess that our results remain good ones notwithstanding the complexity of our cases study.
- It is clear from Table 2 that our approach has allowed us to save a remarkable computational time. For example, if we take the case (N=50), there are 150 calls of exact function evaluations and 788 ones for approximated function, respectively, which present 16% and 84% of the total function calls used in our approach, but at the same time, we note that only this 16% of total calls take 99% of the total computing time required. This last remark explains the idea why we chose not to apply roughly the NBI method with exact evaluations to solve this industrial case.
- Fig. 13 and Table 3 show the profiles (1) and (3) which had the best optimized value for the second criterion (FR_{34}) and the first criterion (VM) respectively.
- Our main goal was to look for new profiles for the twist beam satisfying some requirements (FR_{34} higher and VM smaller than the initial shape ones value), a goal that we achieve successfully (Fig. 13 new profiles (2) and (3)).
- We eliminate all dominated points by a filter, and we remarked that all remaining solutions are almost located at the boundary of the space formed by the elements of the RBF database (Fig. 12). Then we can conclude that the solutions obtained are likely NBI solutions and our approach is able to solve the industrial problem with a reasonable computation time.

Finally, we present a new profile of the automotive twist beam obtained by the shape optimization done by our algorithm (Fig. 14).

4. Conclusion

In this paper, we solved an industrial multicriteria optimization problem namely the shape optimization of an automotive twist beam, the resolution is done by a developed method for the capture of the Pareto front with a reasonable calculation time compared to conventional methods. This method is a coupling between the NBI method and the RBF metamodel which allows us to identify a set of non-dominated solutions well distributed on the Pareto front, and among these solutions, there are some ones that dominate the initial solution (the original design of the twist beam). Similarly, it should be noted that the FFD RBF technique used for deformation and construction of the 3D shape during the optimization process allows us to generate a set of new designs of the automotive twist beam that remain excellent for the industrial partner.

Conflict of interest

None declared.

Acknowledgments

References

[1] Scott R, Sederberg W, Thomas W. Free form deformation of solid geometric models. *SIGGRAPH Computer Graphics (ACM)* 1986;**20**(4) 151–60.

[2] Barr AH. Global and local deformations of solid primitives. *SIGGRAPH Computer Graphics* 1984;**18**(3)21–30.

[3] Coquillart S. Extended free-form deformation: *a sculpturing tool for 3D geometric modeling. SIGGRAPH Computer Graphics (ACM)* 1990;**24**(4) 187–96.

[4] Petroski H. The Anagram was Given in Alphabetical Order, Ceiiinossst-tuv, Representing Ut tensio, sic vis—As the Extension, so The Force: Invention by Design: How Engineers Get from Thought to Thing. Cambridge, MA: Harvard University Press; 1996. p. 11. ISBN 0674463684.

[5] Milton W, Graeme W. The Theory of Composites, Cambridge Monographs on Applied and Computational Mathematics. Cambridge University Press; 2002. ISBN 9780521781251.

[6] Tan SC. Stress Concentrations in Laminated Composites. Lancaster, PA: Technomic Publishing Company; 1994.

[7] Das I, Dennis J. Normal boundary intersection: *a new method for generating Pareto optimal points in multicriteria optimization problems. SIAM Journal on Optimization* 1996;**8**:631–57.

[8] Ganesana T, Vasantb P, Elamvazuthic I. Normal boundary intersection based parametric multi-objective optimization of green sand mould system. *Journal of Manufacturing Systems* 2013;**32**:197–205.

[9] Siddiqui S, Azarm S, Gabriel SA. On improving normal boundary intersection method for generation of pareto frontier. *Structural and Multidisciplinary Optimization* 2012;**46**:839–52.

[10] Das I, Dennis J. Normal Boundary Intersection: An Alternate Method for Generating Pareto Optimal Points in Multicriteria Optimization Problems. NASA contractor report, NASA CR-201616; 1996. p. 38–40.

[11] Wang GG, Shan S. Review of metamodelling techniques in support of engineering design optimization. *ASME J. Mech. Des.* 2007;**129**:370–80.

[12] Praveen C, Duvigneau R. Radial Basis Functions and Kriging Metamodels for Aerodynamic Optimization. INRIA report, RR-6151; 2007. p. 26–30.

[13] Park J, Sandberg JW. Universal approximation using radial basis functions network. *Neural Computation* 1991;**3**:246–57.

[14] Fornberg B, Driscoll TA, Wright GB, Charles R. Observations on the behavior of radial basis functions near boundaries. *Computers & Mathematics with Applications* 2002;**43**:473–90.

[15] Buhmann MD. Radial basis functions. *Acta Numerica* 2000;**9**:19–38.

[16] Tahk MJ, Hong YS, Lee H. Acceleration of the convergence speed of evolutionary algorithms using multilayer neural networks. *Engineering Optimization* 2003;**35**:91–102.

[17] Fang H, Rais-Rohani M, Liu Z, Horstemeyer MF. A comparative study of metamodeling methods for multiobjective crashworthiness optimization. *Computers and Structures* 2005;**83**:2121–36.

[18] Jones R. A taxonomy of global optimization methods based on response surfaces. *Journal of Global Optimization* 2001;**21**:345–83.

[19] Tahk MJ, Hong YS, Lee H. Acceleration of the convergence speed of evolutionary algorithms using multilayer neural networks. *Engineering Optimization* 2003;**35**:91–102.

[20] Sobester A, Leary SJ, Keane AJ. On the design of optimization strategies based on global response surface approximation models. *Journal of Global Optimization* 2005;**33**:31–59.

[21] Lassila T, Rozza G. Parametric free-form shape design with PDE models and reduced basis method. *Computer Methods in Applied Mechanics and Engineering* 2010;**199**:1583–92.

[22] Manzoni A, Quarteroni A, Rozza G. Shape optimization for viscous flows by reduced basis methods and free-form deformation. *International Journal for Numerical Methods in Fluids* 2012;**70**:646–70.

[23] Jacobson A, Baran I, Kavan L, Popovic J, Sorkine O. Fast automatic skinning transformations. *SIGGRAPH* 2012;**30**.

[24] Silveira ME, de Vasconcelos LS, Christoforo A. Numerical simulation of the kinematic behavior of a twist beam suspension using finite element method. *Journal of Mechanical Engineering and Automation* 2012;**2**(6) 150–8.

[25] Benki A, Habbal A, Gael M, Beigneux O. Multicriteria shape design of an aerosol can. Journal of Computational Design and Engineering, http://dx.doi.org/10.1016/j.jcde.2015.03.003.

[27] Deb K. *Multi Objective Optimization using Evolutionary Algorithms.* John Wiley and Sons; 2001. ISBN: 978-0-471-87339-6.

[28] Gopalakrishinan V, Zukoski CF. Delayed flow in thermo-reversible colloidal gels. *Journal of Rheology, Society of Rheology, U.S.A.* 2007; 623–644.

[29] Kim WH, Laird C. Crack nucleation and state I propagation in high strain fatigue-II mechanism. *Acta Metallurgica* 1978;789–99.

[30] Bathias C. There is no infinite fatigue life in metallic materials. *Fatigue & Fracture of Engineering Materials & Structures* 1999;**22**(7)559–65.

[31] von Mises R. Mechanik der festen korper im plastisch deformablen zustand. *Göttingen Nachrichten Mathematisch-Physikalische* 1913;**1**: 582–92.

[32] Huber M. Specific Work of Strain as a Measure of Material Effort, Towarzystwo Politechniczne. Czas. Techniczne, Lwow; 1903.